On the advanced microstructural characterisation of additively manufactured alumina-zirconia based eutectic ceramics

Mainak Saha[1,2]

[1]Department of Metallurgical and Materials Engineering, Indian Institute of Technology Madras, Chennai-600036

[2]Department of Metallurgical and Materials Engineering, National Institute of Technology Durgapur-713209

Corresponding author: Mainak Saha

Email address (es): mainaksaha1995@gmail.com

Phone number: +918017457062

ORCID: Mainak Saha: 0000-0001-8979-457x

Abstract

Due to the outstanding creep and oxidation resistance of alumina-zirconia-based (Al2O3-ZrO2) eutectic ceramics, as well as their superior microstructural stability, there has recently been interest in the production of eutectic ceramics using laser additive manufacturing (AM) techniques. Furthermore, it has been reported that various interesting microstructural features are formed (in these materials) by varying the process parameters, especially the laser scanning speed, associated with the above AM processes. This review paper provides an overview of the current state of research in the field of laser-AM-AZ based eutectic ceramics and highlights the challenges and prospects of this research direction. In addition, the need for correlative microstructural characterization of these materials was highlighted in the perspectives section.

Keywords: Al_2O_3-based eutectic ceramics, Additive Manufacturing, Scanning Transmission Electron Microscopy, Correlative characterisation.

1. Introduction

Alumina-based (Al2O3) ceramics are widely used in industry due to their many beneficial properties, especially low density, high compressive strength, wear resistance, electrical and thermal insulation [1]. Al2O3 ceramic is a potential candidate for dental and orthopedic applications due to its high purity material and good printing properties and biocompatibility [2]. On the other hand, the layer-by-layer deposition of the materials used in laser additive manufacturing (AM) results in large-scale microstructural inhomogeneities and crack formation in the deposited layers due to thermal stress [3]-[12]. However, the (deposited) material must have good fracture toughness to prevent cracking during layered deposition [3], [13]-[16]. Al2O3 ceramic. Its main drawback is its low fracture toughness, which precludes the use of his laser-based AM technique [1]. Addition of zirconia (ZrO2) to Al2O3 ceramics has proven to be an effective method of increasing fracture toughness (for AM-based samples) through crack bridging and deflection mechanisms. The effect of ZrO addition to AM-based His Al2O3 was

reported by Pappas et al. explained. [1] Uses a laser direct deposition process. Li and Zhang [17] studied the microstructure of Al2O3-ZrO2 (AZ) ceramics with ZrO2 concentrations above 35 wt% by direct laser deposition. According to Wilkes et al. [18], AZ ceramics can be successfully fabricated without microcracks by preheating each layer (using a CO2 laser beam). Homeny and Nick [19] studied the relationship between the eutectic ceramic structure and the properties of his AZ-Y2O3. The stabilization of ZrO2 lamellae in rapidly formed eutectic AZ ceramics was studied by Moreno and Yoshimura [20]. Addition of zirconia (ZrO2) to Al2O3 ceramics has proven to be an effective method of increasing fracture toughness (for AM-based samples) through crack bridging and deflection mechanisms. The effect of ZrO addition to AM-based His Al2O3 was reported by Pappas et al. explained. [1] Uses a laser direct deposition process. Li and Zhang [17] studied the microstructure of Al2O3-ZrO2 (AZ) ceramics with ZrO2 concentrations above 35 wt% by direct laser deposition. Wilkes et al. [18] reported that preheating each layer (using a CO2 laser beam) can eliminate microcracks in AZ ceramics. Homeny and Nick [19] studied the structure-property correlation of AZ-Y2O3 eutectic ceramics. Moreno and Yoshimura [20] studied the stabilization of ZrO2 lamellae in rapidly solidified AZ eutectic ceramics. The microstructure and physical properties of directionally solidified AZ eutectic ceramics were reported by Trnovcova et al. [21]. By introducing his three recent works in this field, this article aims to provide an overview of the current state of research in the field of eutectic ceramics based on his Laser-AM AZ. Short future prospects in this direction were also highlighted at the end of the article.

2. Relevant topics

2.1 Characterization of colonial boundaries in laser-directed energy deposition-fabricated AZ-GdAlO3 eutectic ceramic

The microstructure of eutectic AZ-GdAlO3 ceramics fabricated by LDED (Laser Directed Energy Deposition) technique was reported by Liu et al. Examined. [twenty two]. The formation of periodic stripes in the building direction (BD) has been shown, which is attributed to the anomalous growth of nanoscale structures along the weld pool [22]. A “kanji” eutectic structure is found within the eutectic colony [22], intersecting the light (GdAlO3) and dark (Al2O3) phases. It was also noted that the longitudinal section of the colony has a cylindrical morphology and extends perpendicular to the BD [22]. The heat transfer behavior within the melt pool that grows the microstructures against the heat flow is mainly due to the colony shape (longitudinal section) mentioned above. Furthermore, the eutectic distance was found to decrease from ~0.63 ± 0.11 μm at the sample surface to ~0.99 ± 0.08 μm in the center of the sample [22]. This is explained by faster cooling at the surface than inside the sample [22]. A concave band can be seen along the BD in Fig. 1(a). Colonial boundaries can be clearly seen in

the various levels of the cladding layer microstructure based on scanning electron microscopy (SEM) shown in Fig. 1(b)-(d).

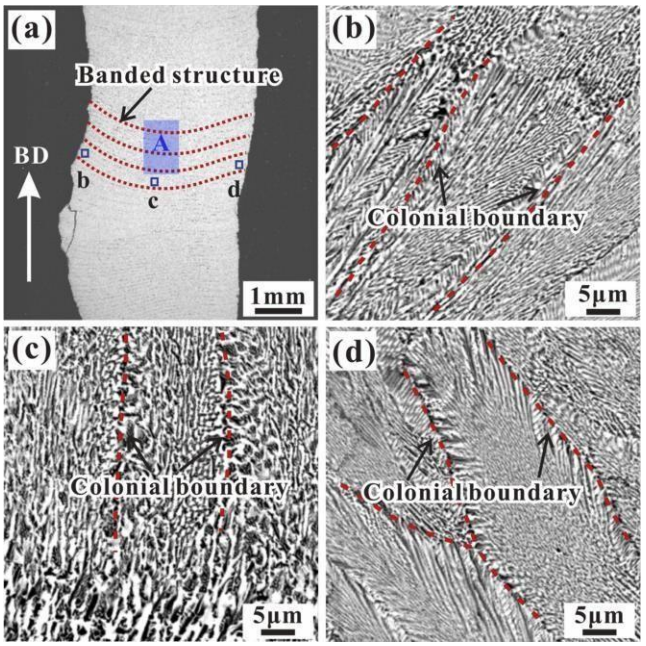

Fig. 1 SEM micrographs (of the longitudinal section) of the AZ-$GdAlO_3$ eutectic ceramic: (a) periodic banded structure, (b) Left side of a deposited layer, (c) Centre of a deposited layer, and (d) Right side of a deposited layer [22].

2.2 Microstructure obtained during solidification of selective laser melted AZ-$GdAlO_3$ eutectic ceramic

The effect of laser scanning speed on the strengthening of AZ-GdAlO3 eutectic ceramics during selective laser melting (SLM) technique was reported by Liu et al. report. Examined. [23]. It was found that the relative density of the solidified sample decreased from 98.7% to 95.7% when the laser scanning speed was increased to 48 mm/min [23]. It was observed that both melt width and melt depth decreased with increasing scan speed. This is further evidence that conduction is the most important heat transfer mechanism associated with the solidification process [23]. An interesting finding is that the eutectic distance at the top of the weld pool first decreases from 6 mm/min to 12 mm/min with increasing laser scan speed, and then decreases to 12 mm/min with increasing laser scan speed. is to increase to Max 48mm/min. speed [23]. The above relationship between eutectic distance and scanning speed was explained by the change of the solidification rate determinant from laser scanning speed to the angle between the scanning direction and the microstructure growth direction [16], [23]. At scan speeds below 12 mm/min, quenching has been observed to induce microcracks and increase surface roughness (due to abrasion effects and the presence of microstructural pores) [23]. Furthermore, it has been reported that solidification defects are reduced when the laser scanning speed is less than 12 mm/min [23].

2.3 Nanostructured AZ-YAG fabricated using laser engineered net shaping technique

Using the LENS method, Fan et al. [24] reported the fabrication of highly dense (98%) thin-walled Al2O3-YAG-ZrO2 (AYZ) eutectic ceramics. The three phases, namely -Al2O3, YAG, and ZrO2-, interpenetrate in the as-synthesized state of the material and exhibit a cellular microstructure [24]. A morphology change from planar to cellular eutectic microstructure (along the BD) was also observed in

each deposited layer [24]. Images of his as-fabricated AYZ ceramics taken with scanning transmission electron microscopy (STEM) and high angle ring dark field (HAADF) are shown in the Fig. 2(a) [24]. Matched energy dispersive spectroscopy (EDS) STEM maps of Al, Y, Zr, and O are shown in the Fig. 2(b-e). As is clear from the illustration (Fig. 2(b–e)), the dark, gray and bright phases in the STEM-HAADF image (Fig. 2(a)) correspond to -Al2O3, YAG and cubic ZrO2 phases. Moreover, as seen in the illustration (Fig. 2(b–e)), Y2O3 is dissolved in ZrO2 in the as-produced state, indicating that cubic ZrO2 is stabilized by Y^{3+} during solidification (during LENS). [24].

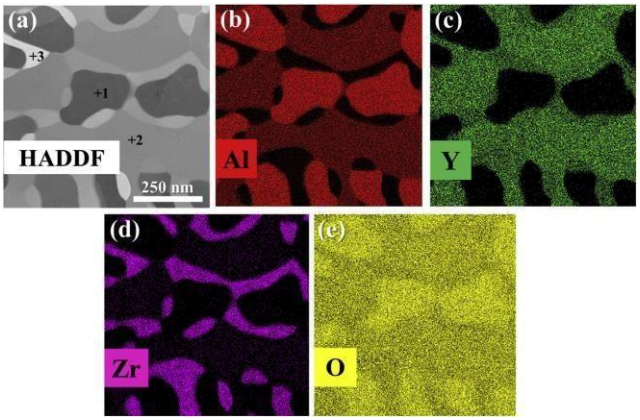

Fig. 2 AYZ: **(a)** STEM-HAADF image, and corresponding STEM-EDS maps of **(b)** Al, **(c)** Y, **(d)** Zr, and **(e)** O [24]. Points 1, 2 and 3 marked in part **(a)** represent the regions where point EDS mapping has been performed.

A fibrous eutectic structure is also claimed to interpenetrate randomly along the boundaries of the generated samples [24]. This is explained by the significantly faster solidification rate in the edge region compared to the interior of the sample [24]. Furthermore, the orientation relationship between the three phases in the LENSed sample was confirmed using Kikuchi transmission diffraction between 001YAG and 001ZrO2 containing 11-20Al2O3, 0001>Al2O3 // 001>YAG // 001>ZrO2 (only 3.5 ° deviation). (TKD) technique and verified by high-resolution transmission electron microscopy (HRTEM) imaging of the triple junction between the Al2O3, YAG and ZrO2 phases (Fig. 3) [The above differences are due to the growth kinetics and interfacial energy [24]]. For example, the better parallelism of 11-20 Al2O3//001 ZrO2 compared to 11-20 Al2O3//001 YAG [16], [24] and the lower interfacial energy of the Al2O3/ZrO2 interface (0.74 J/m2) compared to the Al2O3/YAG interface with an interfacial energy of 3.23 J/m2 [24].

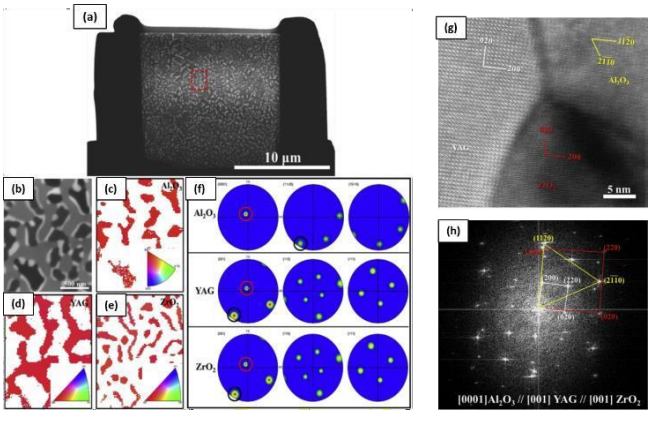

Fig. 3 AYZ shows the following images: (a) SEM image of the electron transparent lamella of the transverse section of the LENSed specimen created using the Focused Ion Beam (FIB)-based liftout technique; (b) SEM image of the region of interest for TKD mapping inside the cellular eutectic; (c), (d), and (e) TKD-based inverse pole figure (IPF) maps of Al2O3, A closer look at the area that was highlighted using a red-dotted rectangle in part **(a)** has been shown in part **(b)**.

A longitudinal segment of a LENSed AYZ sample with TKD analysis along the BD is shown in Fig. 4 using SEM images [24]. The cell eutectic growth direction is <0001>Al2O3 // <001>YAG // <001>ZrO2 [24], which is the same as for the cross section of the AYZ sample. In the longitudinal section, YAG crystals with moderate growth direction can be seen [24] in contrast to the cross section. This can be explained by the fact that these crystals (found mainly at cell boundaries as in Fig. 1) are present. 4) deviating from the customary plane and walking in the direction of cell elongation rather than parallel to it; Sayle and Farmer [25] and Milenkovic Both [26] reported similar observations for Al2O3-ZrO2 and Ni-Al-V cellular eutectic alloys, respectively.

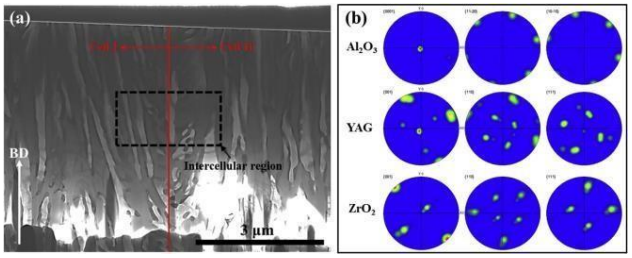

Fig. 4 AYZ shows (a) a SEM picture of the electron transparent lamella of the longitudinal slice of the LENSed specimen created utilising the TKD-based Focused Ion Beam (FIB)-based liftout approach, and (b) the pole figures of -Al2O3, -YAG, and -ZrO2 [24]. In part (a), a block-dotted rectangular box encloses the intercellular region from which the pole figures in part (b) were derived. BD abbreviates for building direction in section (a).

3. Future directions

This article briefly reviews the current state of research on AM laser-AM-based AZ ceramics. The current goal (in this direction) is to improve the microstructure (in several process parameters related to AM-based production methods) so that these ceramic materials are mechanically better than materials produced by conventional methods. optimization). The characterization of different interfaces, especially eutectic boundaries, in that context has not yet been addressed in eutectic ceramics (especially AZ ceramics). For example, the case study described in Chapter 4 is (so far) the only one that has been able to obtain electron-transparent laminates in both transverse and longitudinal sections using the FIB-based flow-through technique on AYZ ceramics. is a study to determine the relationships between individual phases (-Al2O3, YAG and ZrO2) using the TKD technique. This applies to AM laser-based AZ

ceramics as well as other laser-based materials. Grain boundary engineering (GBE) for both metallic and ceramic materials is based on the replacement of high-energy random high-angle GBs (HAGBs) of various materials with low-energy random high-angle GBs (HAGBs). It has evolved over the past 40 years. function optimizing technology. Energy GB [27], [28]. GBEs have been described as a mechanism to replace normal HAGBs with special (low-energy) HAGBs, also called coincident lattice boundaries (CSLs), which are more common in metallic materials with cubic crystal structures [29]–[32]. . The whole GBE approach is based on reducing the total energy of the GB microstructure so that the 2D interfaces (GB and IB) are resistant to corrosion, oxidation, irregular grain development and intergranular fracture. I am here. In addition, thermomechanical processing (TMP) is the most common method to fabricate GBE microstructures in most metallic materials [33]. The existence of low-energy CSL barriers is difficult to imagine because CSL theory does not work in ceramics with more complex crystal structures [34]–[36]. In addition, the low strength of ceramics prevents the use of processes (especially TMP) used in metallic materials to create GBE microstructures at both room and high temperatures. Therefore, it is very difficult to create a GBE microstructure in AZ ceramics.

4. Summary and conclusion

Correlative microscopy [37], [38] is one of the recently developed approaches to link the structure of GBs and interfacial barriers (IBs) with local composition at the atomic level (in polycrystalline materials). This methodology is widely used, especially in the context of metallic materials, to study the structure and composition of GBs, as well as the five macroscopic and three microscopic degrees of freedom (DOFs) (of GBs and IBs). used. However, there are still few studies on microstructural correlations related to AZ ceramics. The complexity of the crystal structure and sample preparation may be the reason. Moreover, as outlined in section 1, layer-by-layer material deposition is the basis of laser AM-based processes. The complexity (regarding the creation of GBE microstructures) increases with the emergence of large-scale microstructural inhomogeneities (with high defect concentrations) [39] and non-equilibrium microstructures. Consequently, the ability to fabricate his GBE microstructures in AM-based AZ ceramics opens up many possibilities for subsequent AZ ceramics research.

References

[1] J. M. Pappas, A. R. Thakur, and X. Dong, “Effects of zirconia doping on additively manufactured alumina ceramics by laser direct deposition,” *Mater Des*, vol. 192, p. 108711,Jul. 2020, doi: 10.1016/j.matdes.2020.108711.

[2] V. K. Balla, S. Bose, and A. Bandyopadhyay, “Processing of bulk alumina ceramics using laser engineered net shaping,” *Int J Appl Ceram Technol*, vol. 5, no. 3, pp. 234–

242, May 2008, doi:10.1111/j.1744-7402.2008.02202.x.

[3] C. K. Chua, K. F. Leong, and J. An, "Additive Manufacturing and 3D Printing," in *Biomedical Materials*, Springer International Publishing, 2021, pp. 621–652. doi: 10.1007/978-3-030- 49206-9_19.

[4] O. Abdulhameed, A. Al-Ahmari, W. Ameen, and S. H. Mian, "Additive manufacturing: Challenges, trends, and applications," *Advances in Mechanical Engineering*, vol. 11, no. 2,Feb. 2019, doi: 10.1177/1687814018822880.

[5] Saha M, Mallik M. Surface engineering of nanomaterials: Processing and applications. InSurface Engineering 2022 Sep 14 (pp. 95-119). CRC Press

[6] M. Saha and M. Mallik, "Additive Manufacturing and Characterisation of Biomedical Materials," *Advanced Materials for Biomechanical Applications*, pp. 29–57, May 2022, doi:10.1201/9781003286806-3.

[7] M. Saha and M. Mallik, "Metal-based conducive nano-inks: synthesis and characterization techniques," *Smart Multifunctional Nano-Inks*, pp. 27–52, Jan. 2023, doi: 10.1016/B978-0-323-91145-0.00003-7.

[8] M. Saha, "3D printing of nanoceramics: Present status and future perspectives," Sep. 2022,doi: 10.48550/arxiv.2210.06948.

[9] M. Saha, "Fly ash composites: A review," Feb. 2022, doi: 10.48550/arxiv.2202.11167.

[10] M. Saha, "Grain boundary segregation in steels: Towards engineering the design of internalinterfaces," Feb. 2022, doi: 10.48550/arxiv.2202.12971.

[11] M. Saha, "New frontiers in characterising ZrB$_2$-MoSi$_2$ ultra-high temperature ceramics," Feb. 2022, doi: 10.48550/arxiv.2202.11162.

[12] M. Saha, "On the advanced microstructural characterisation of additively manufactured alumina-zirconia based eutectic ceramics: Overview and outlook," Dec. 2022, doi: 10.26434/CHEMRXIV-2022-84LD6.

[13] W. E. Frazier, "Metal additive manufacturing: A review," *Journal of Materials Engineering and Performance*, vol. 23, no. 6. Springer New York LLC, pp. 1917–1928, 2014. doi: 10.1007/s11665-014-0958-z.

[14] A. Zocca, P. Colombo, C. M. Gomes, and J. Günster, "Additive Manufacturing of Ceramics:
Issues, Potentialities, and Opportunities," *Journal of the American Ceramic Society*, vol. 98,no. 7, pp. 1983–2001, Jul. 2015, doi: 10.1111/jace.13700.

[15] A. Vyatskikh, S. Delalande, A. Kudo, X. Zhang, C. M. Portela, and J. R. Greer, "Additive manufacturing of 3D nano-architected metals," *Nat Commun*, vol. 9, no. 1, pp. 1–8, Dec.2018, doi: 10.1038/s41467-018-03071-9.

[16] M. Saha and M. Mallik, "Additive manufacturing of ceramics and cermets: present status and future perspectives," *Sādhanā 2021 46:3*, vol. 46, no. 3, pp. 1–35, Aug. 2021, doi: 10.1007/S12046-021-01685-2.

[17] F. Li and Y. Zhang, " Microstructural characterization of Al 2 O 3 -ZrO 2 ceramic by laser direct material deposition ," *J Laser Appl*, vol. 31, no. 2, p. 022509, May 2019, doi: 10.2351/1.5096125.

[18] J. Wilkes, Y. C. Hagedorn, W. Meiners, and K. Wissenbach, "Additive

manufacturing of ZrO2- Al2O3 ceramic components by selective laser melting," *Rapid Prototyp J*, vol. 19, no. 1, pp. 51–57, 2013, doi: 10.1108/13552541311292736.

[19] J. Homeny and J. J. Nick, "Microstructure-property relations of alumina-zirconia eutectic ceramics," *Materials Science and Engineering A*, vol. 127, no. 1, pp. 123–133, Jul. 1990, doi:10.1016/0921-5093(90)90198-C.

[20] J. M. Calderon-Moreno and M. Yoshimura, "Stabilization of zirconia lamellae in rapidly solidified alumina-zirconia eutectic composites," *J Eur Ceram Soc*, vol. 25, no. 8 SPEC. ISS., pp.1369–1372, Jan. 2005, doi: 10.1016/j.jeurceramsoc.2005.01.013.

[21] V. Trnovcovfi, M. Starostin, V. Labas, and R. Cicka, "Microstructure and Physical Properties of Directionally Solidified Alumina-Zirconia Eutectic Composites," 1998.

[22] H. Liu *et al.*, "One-step additive manufacturing and microstructure evolution of melt-grown Al2O3/GdAlO3/ZrO2 eutectic ceramics by laser directed energy deposition," *J Eur Ceram Soc*, vol. 41, no. 6, pp. 3547–3558, Jun. 2021, doi: 10.1016/j.jeurceramsoc.2021.01.047.

[23] H. Liu *et al.*, "Effect of scanning speed on the solidification process of Al2O3/GdAlO3/ZrO2 eutectic ceramics in a single track by selective laser melting," *Ceram Int*, vol. 45, no. 14, pp. 17252–17257, Oct. 2019, doi: 10.1016/j.ceramint.2019.05.281.

[24] Z. Fan *et al.*, "Nanostructured Al 2 O 3 -YAG-ZrO 2 ternary eutectic components prepared by laser engineered net shaping," *Acta Mater*, vol. 170, pp. 24–37, May 2019, doi: 10.1016/j.actamat.2019.03.020.

[25] A. Sayir and S. C. Farmer, "Effect of the microstructure on mechanical properties of directionally solidified Al2O3/ZrO2(Y2O3) eutectic," *Acta Mater*, vol. 48, no. 18–19, pp. 4691–4697, Dec. 2000, doi: 10.1016/S1359-6454(00)00259-7.

[26] S. Milenkovic, A. A. Coelho, and R. Caram, "Directional solidification processing of eutectic alloys in the Ni-Al-V system," *J Cryst Growth*, vol. 211, no. 1, pp. 485–490, Apr. 2000, doi: 10.1016/S0022-0248(99)00783-6.

[27] D. Raabe *et al.*, "Grain boundary segregation engineering in metallic alloys: A pathway to the design of interfaces," *Curr Opin Solid State Mater Sci*, vol. 18, no. 4, pp. 253–261, 2014, doi: 10.1016/j.cossms.2014.06.002.

[28] Y. Ikuhara, "Grain boundary and interface structures in ceramics," *Journal of the Ceramic Society of Japan*, vol. 109, no. 1271. Ceramic Society of Japan, pp. S110–S120, Jul. 01, 2001.doi: 10.2109/jcersj.109.1271_S110.

[29] A. D. Rollett, "Texture development dependence on grain boundary properties," in *Materials Science Forum*, 2002, vol. 408–412, no. I, pp. 251–256. doi: 10.4028/www.scientific.net/msf.408-412.251.

[30] M. Winning and A. D. Rollett, "Transition between low and high angle grain boundaries," *Acta Mater*, vol. 53, no. 10, pp. 2901–2907, Jun. 2005, doi: 10.1016/j.actamat.2005.03.005.

[31] D. Brandon, "25 Year Perspective Defining grain boundaries: An historical perspective the development and limitations of coincident site lattice models," *Materials Science and Technology*, vol. 26, no. 7. pp. 762–773, Jul. 01, 2010. doi: 10.1179/026708310X12635619987989.

[32] D. G. Brandon, “The structure of high-angle grain boundaries,” *Acta Metallurgica*, vol. 14, no.11, pp. 1479–1484, 1966, doi: 10.1016/0001-6160(66)90168-4.

[33] W. M. Ashmawi and M. A. Zikry, “Prediction of grain-boundary interfacial mechanisms in polycrystalline materials,” *Journal of Engineering Materials and Technology, Transactions of the ASME*, vol. 124, no. 1, pp. 88–96, 2002, doi: 10.1115/1.1421611.

[34] V. Y. Gertsman, A. P. Zhilyaev, and J. A. Szpunar, “Grain boundary misorientation distributions in monoclinic zirconia,” *Model Simul Mat Sci Eng*, vol. 5, no. 1, pp. 35–52, Jan. 1997, doi: 10.1088/0965-0393/5/1/003.

[35] H. Grimmer, “Coincidence-site lattices,” *Acta Crystallographica Section A*, vol. 32, no. 5, pp.783–785, Sep. 1976, doi: 10.1107/S056773947601231X.

[36] A. P. Sutton, R. W. Balluffi, and V. Vitek, “On intrinsic secondary grain boundary dislocation arrays in high angle symmetrical tilt grain boundaries,” *Scripta Metallurgica*, vol. 15, no. 9, pp.989–994, 1981, doi: 10.1016/0036-9748(81)90240-4.

[37] Y. Toji, H. Matsuda, M. Herbig, P. P. Choi, and D. Raabe, “Atomic-scale analysis of carbon partitioning between martensite and austenite by atom probe tomography and correlative transmission electron microscopy,” *Acta Mater*, vol. 65, pp. 215–228, Feb. 2014, doi: 10.1016/j.actamat.2013.10.064.

[38] C. H. Liebscher *et al.*, “Tetragonal fcc-Fe induced by κ -carbide precipitates: Atomic scale insights from correlative electron microscopy, atom probe tomography, and density functional theory,” *Phys Rev Mater*, vol. 2, no. 2, pp. 1–6, 2018, doi: 10.1103/PhysRevMaterials.2.023804.

[39] M. Schwentenwein and J. Homa, “Additive manufacturing of dense alumina ceramics,” *Int J Appl Ceram Technol*, vol. 12, no. 1, pp. 1–7, Jan. 2015, doi: 10.1111/ijac.12319.